

Self-Assembly and Self-Organization of Self-Recognizing Cyclophanes

Peter R. Ashton^a, Alexandre Chemin^a, Christian G. Claessens^a, Stephan Menzer^b, J. Fraser Stoddart^{*a[†]}, Andrew J. P. White^b, and David J. Williams^bSchool of Chemistry, University of Birmingham,^a
Edgbaston, Birmingham B15 2TT, UKDepartment of Chemistry, Imperial College,^b
South Kensington, London SW7 2AY, UK
Fax: (internat.) +44(0)171/594-5804

Received December 12, 1997

Keywords: Crystal engineering / Host-guest chemistry / Nanotubes / Sandwich complexes / Self-assembly

An analysis is presented of the different contributions that give rise to the packing observed in the crystal structures of a wide range of bipyridinium-based molecular assemblies and supramolecular arrays. It is demonstrated how the various interactions – electrostatic, van der Waals, and π - π interactions – that contribute to the solid-state arrangement of these molecules and supermolecules can be utilized in order to design a series of tetracationic cyclophanes that can potentially self-organize in a highly ordered way in the solid state by virtue of the fact that they contain π -electron donors as well as π -electron acceptors. The syntheses of these cyclophanes is outlined and the tunability of the self-assembly methodology in their construction is demonstrated. One of these tetracationic cyclophanes – comprising π -electron-rich hydroquinone rings and π -electron-deficient bipyridinium units – has been shown to pack as highly

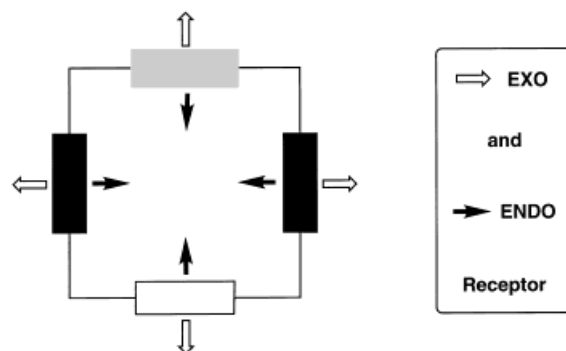
ordered two-dimensional, mosaic-like sheets in the solid state. Its dicationic precursor also forms extended π - π -stacked layers in the solid state. An analogous cyclophane – containing two π -electron-rich resorcinol rings in place of the two hydroquinone rings – forms, in the solid state, one-dimensional arrays wherein the component resorcinol rings interact through their parallel π - π stacking. It has also been established that the first of the aforementioned tetracationic cyclophanes forms a 1:1 adduct with ferrocene in both the solution and solid states. X-ray crystallography, performed on the 1:1 adduct, reveals that not only is the ferrocene molecule complexed in a π - π stacking sense within the tetracationic cyclophane, but the 1:1 adduct also packs in a manner that is remarkably similar to the supramolecular organization of the free cyclophane in the crystalline state.

Introduction

Self-assembly processes have been employed^[1] successfully to build with accuracy molecular assemblies and supramolecular arrays formerly unattainable using conventional chemistry. Hydrogen bonding,^[2] metal-ligand complexation^[3] and π - π stacking^[4] recognition motifs have been employed rationally to design and, to some extent, realize one-, two-, and three-dimensional solid-state arrays and networks.^[5] The creation of a new generation of functioning materials depends ultimately on the development of molecular and supramolecular architectures exhibiting novel properties.^[6] A more fundamental understanding of the molecular recognition phenomena leading to these proper-

ties is of the utmost importance to the chemist who wishes to develop new organic materials.

Figure 1. A generic cyclophane containing four recognition units that can act as both an *endo* and an *exo* receptor; the two black rectangles represents two identical interacting units; the white and grey rectangles represents two interacting units that can be either identical or different



From a careful examination of the solid-state structures of a wide range of bipyridinium-based molecular compounds, we have been able to identify some of the major

^[◇] Part 36: D. B. Amabilino, M. Asakawa, P. R. Ashton, R. Ballardini, V. Balzani, M. Belohradsky, A. Credi, M. Higuchi, F. M. Raymo, T. Shimizu, J. F. Stoddart, M. Venturi, K. Yase, *New J. Chem.*, submitted.

^[†] Current correspondence address: Department of Chemistry and Biochemistry, University of California at Los Angeles, 405 Hilgard Avenue, Los Angeles, CA 90095-1569, USA; Fax: (internat.) + 1-310/206-1843; E-mail: stoddart@chem.ucla.edu

interactive patterns that govern their packing. Armed with this information, we have designed (Figure 1) a series of cyclophanes in which either two π -electron-rich or two π -electron-neutral rings, together with two π -electron-deficient bipyridinium units, are placed in diametrically opposite positions within the same molecule so as to create a box-like molecular geometry. These features give these cyclophanes the potential to form highly structured two-dimensional arrays of stacked π - π -interacting aromatic units after a mosaic-like fashion, while they still retain the ability to bind either π -electron-rich or π -electron-deficient substrates.

Here, we report on (i) the design and self-assembly of nine tetracationic cyclophanes **4–12**·4 PF₆, (ii) the X-ray crystallographic characterization of two (**4**·4 PF₆ and **8**·4 PF₆) of them, as well as of one dicationic precursor **15**·2 PF₆, and (iii) the ability of the cyclophane **4**·4 PF₆ to form a 1:1 adduct with ferrocene which has been characterized in both the solid and solution states.

Results and Discussion

Design

In order to design, as rationally as possible, cyclophanes with the potential for self-recognition, a knowledge of the interactions that control their self-organization in the solid state is required.

(E) = Electrostatic Interactions

The compounds we will be considering are all salts and therefore the first, strong, short contact interactions that govern their packing are electrostatic. These interactions are probably the major contributors to the primary structures in the packing of most of the charged species, synthesized and characterized in our own research laboratories during the last decade.

(CP) = Close Packing Considerations

The visualization of a molecule as a collection of spherical atoms, with their characteristic radii, results inevitably in the concept of close packing of molecules in a crystal. This model, described in 1945 by Kitaigorodskii,^[7] is based on the fact that the number of intermolecular contacts in a crystal tends to a maximum, and that these contacts cluster around distances associated with energy minima in the various atom-atom potential curves. The close packing principle applies to a far lesser extent than do the electrostatic interactions in the case of the ionic species we are considering, but it certainly does contribute to their secondary structure along with the other interactions described below.

(π) = π - π Interactions

Many different types of aromatic units have been incorporated into bipyridinium-based molecular systems. In Figure 2, we list all the different types of π - π interactions encountered to date and comment on their effect on packing. We identify the dioxy-substituted aromatic ring systems as

being π -electron-rich, the dialkyl-substituted ones as π -neutral, and the bipyridinium units as π -electron-deficient.

(π -1) π -Electron-Rich– π -Electron-Deficient: The interaction between a π -electron-deficient aromatic unit, such as the 4,4'-bipyridinium dication, and a π -electron-rich moiety, such as a hydroquinone or 1,5-dioxynaphthalene ring system, is (Figure 2b) the most recurrent form of aromatic-aromatic stacking observed in solid-state structures of bipyridinium-based molecular compounds.^{[8][9][10]} This interaction is responsible for the formation, in the solid state, of both one-^{[8][9]} and two-^[10]dimensional superstructures. To date, the presence of counterions has rendered impossible the making of three-dimensional networks, comprising solely π - π interacting units.

(π -2) π -Electron-Rich– π -Electron-Rich: Close packing has been observed between benzofuran-based ring systems^[11], as well as between hydroquinone or 1,5-dioxynaphthalene aromatic rings.^[12] This interaction alone has been found to be responsible for the formation, in the solid state, of zero-^[11] and one-^[12]dimensional structures.

(π -3) π -Electron-Deficient– π -Electron-Deficient: This type of interaction has been found in two different contexts: (i) when the bipyridinium units of two adjacent molecules are aligned and facing each other,^[13] and (ii) when one of the pyridinium rings of a 4,4'-bipyridinium unit in one molecule is (Figure 2a) π - π interacting with another one in an adjacent molecule in a parallel fashion.^[14] π - π Interactions between bipyridinium units is, at first glance, a rather surprising phenomenon since it implies the close contact between two positively charged species.

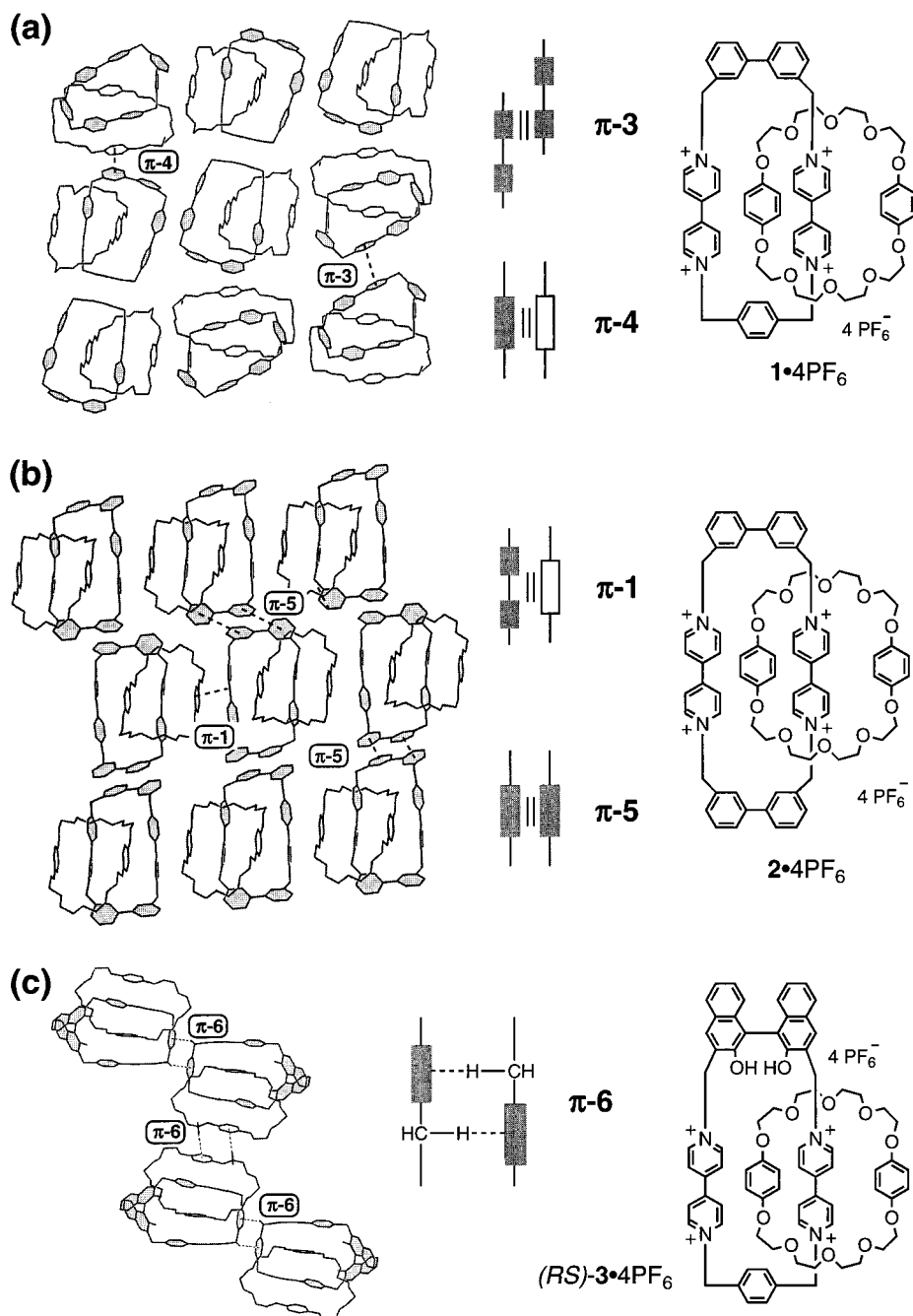
(π -4) π -Electron-Rich– π -Neutral: The solid-state structures of some catenanes^[10a] and pseudorotaxanes^[10b] reveal (Figure 2a) a close packing between the π -neutral spacer of a tetracationic cyclophane and a π -electron-rich aromatic unit in an adjacent molecule.

(π -5) π -Neutral– π -Neutral: In several cases, when the spacers of a tetracationic cyclophane are either 4,4'-^[13] or 3,3'-^[14]biphenyl units, π -neutral– π -neutral interactions have been observed (Figure 2b) between adjacent tetracationic cyclophanes. The same two interaction patterns, analogous to the ones described in π -3 for the case of the π -electron deficient– π -electron deficient interaction, have been found in the solid state.

(π -6) CH– π : These interactions have been described (Figure 2c), for example, in bipyridinium-based systems and this was in the case of a [2]catenane.^[14]

In the knowledge of these interactive patterns, a series of tetracationic cyclophanes incorporating a variety of potentially interactive π - π units that, in all cases, contain two 4,4'-bipyridinium units located diametrically opposite one another, has been designed. The major contributor to their packing – as stated above – is the electrostatic interaction (E). Another contribution, which is not insignificant, concerns the shapes of the molecules that contribute to their arrangements in a close-packing (CP) sense. To illustrate this point, let us quote Desiraju,^[5e] who wrote: "...chemistry is not geometry, and the major challenge in the practice of crystal engineering is that a crystal structure is a compromise,

Figure 2. Parts of the continuous two-dimensional stacks formed by the [2]catenanes $1 \cdot 4 \text{ PF}_6$, $2 \cdot 4 \text{ PF}_6$, and $(RS)\text{-}3 \cdot 4 \text{ PF}_6$ showing the interactive patterns a) $\pi\text{-}3$ and $\pi\text{-}4$, b) $\pi\text{-}1$ and $\pi\text{-}5$, and c) $\pi\text{-}6$ in the solid state and in a schematic way



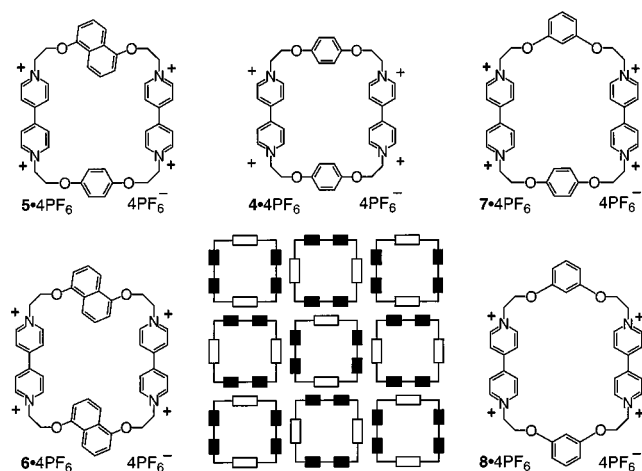
at times quite uneasy, between interactions of varying strengths, directionalities, and distance-dependent properties.”

The incorporation of two π -electron-rich ring systems and two 4,4'-bipyridinium units located diametrically opposite each other in the same tetracationic cyclophane, creating a box-like geometry, provides the potential to form, in the solid state, a highly ordered two-dimensional array (Figure 3) wherein the superstructure would be sustained by the combination of E, CP, and $\pi\text{-}2$ interactions. The π -electron-rich units selected were hydroquinone in $4 \cdot 4 \text{ PF}_6$,

1,5-dioxynaphthalene in $5 \cdot 4 \text{ PF}_6$ and $6 \cdot 4 \text{ PF}_6$, and resorcinol in $7 \cdot 4 \text{ PF}_6$ and $8 \cdot 4 \text{ PF}_6$ on the basis of their known ability to stack with a π -electron-deficient unit present in another molecule. The length of the π -electron-rich spacer unit is such that the cyclophanes should adopt a near-square geometry in the solid state, a condition that is necessary in order to realize the mosaic-like array depicted in Figure 3.

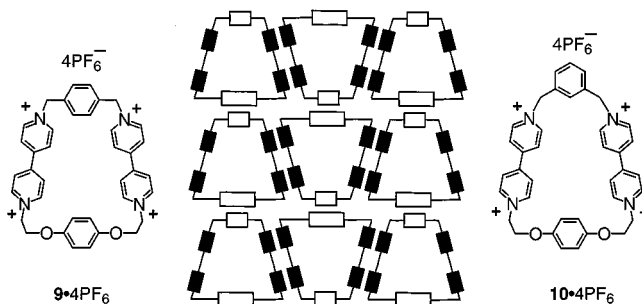
A consideration of the cooperative effect between the four interactions E, CP, $\pi\text{-}3$, and $\pi\text{-}4$ led us to design the

Figure 3. Schematic representation of the anticipated solid-state packing of the tetracations incorporating both π -electron-rich and π -electron-deficient units in a crystalline salt



tetracationic cyclophanes $9 \cdot 4 \text{ PF}_6$ and $10 \cdot 4 \text{ PF}_6$ with the potential to pack as illustrated in Figure 4. It is anticipated that these cyclophanes will adopt a triangular shape since one of the π -electron-rich hydroquinone rings of the tetracationic cyclophane $4 \cdot 4 \text{ PF}_6$ has been modified to a shorter *p*-xylyl unit in $9 \cdot 4 \text{ PF}_6$ and an even shorter *m*-xylyl unit in $10 \cdot 4 \text{ PF}_6$.

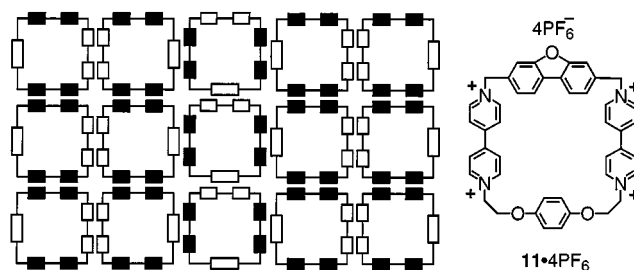
Figure 4. Schematic representation of the anticipated solid-state packing of the tetracations incorporating π -electron-rich, π -neutral, and π -electron-deficient units in a crystalline salt



Dibenzofuran is well known to π - π stack with itself in the solid state.^{[11a][11b][11c]} Two of these units have been incorporated into a tetracationic cyclophane containing also two bipyridinium units located diametrically opposite each other.^[11d] The solid-state structure of this cyclophane revealed the formation of one-dimensional π - π stacks of dibenzofuran interacting units. In the tetracationic cyclophane $11 \cdot 4 \text{ PF}_6$, containing both dibenzofuran and hydroquinone units, the expected packing (Figure 5) relies on the combination of the interactions: E, CP, π -1, π -3, π -4, and π -5.

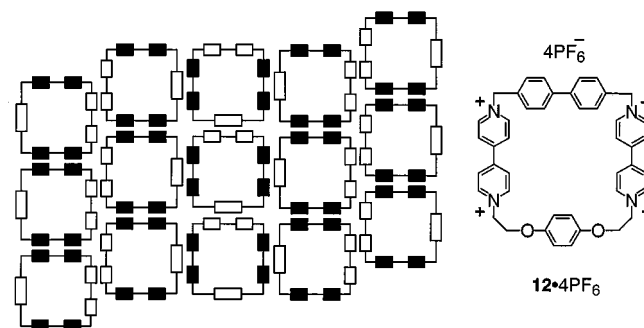
The idea of synthesizing the tetracationic cyclophane $12 \cdot 4 \text{ PF}_6$, in which one of the π -electron rich spacers of $4 \cdot 4 \text{ PF}_6$ has been replaced by the π -neutral biphenyl ring system, derives from the knowledge^[13] of the solid-state structure of the cyclophane cyclobis(paraquat-4,4'-biphenylene) that forms highly ordered layered arrays. The expected

Figure 5. Schematic representation of the anticipated solid-state packing of the tetracation 11^{4+} in a crystalline salt



packing in the solid-state structure of $12 \cdot 4 \text{ PF}_6$ relies (Figure 6) on the combination of the interactions: E, CP, π -1, π -2, π -3, and π -4.

Figure 6. Schematic representation of the anticipated solid-state packing of the tetracation 12^{4+} in a crystalline salt

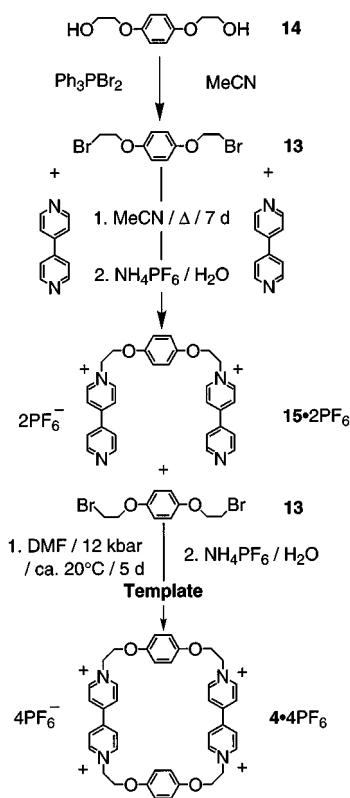


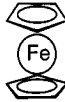
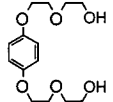
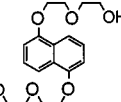
Synthesis

The tetracationic cyclophane $4 \cdot 4 \text{ PF}_6$ was prepared by the route shown in Scheme 1. The dibromide **13** was obtained by reaction^[15] of the diol **14** with PPh_3Br_2 in MeCN. Portion-wise addition of **13** over 7 days to a ten-fold excess of 4,4'-bipyridine in MeCN afforded, after counterion exchange, the dicationic salt $15 \cdot 2 \text{ PF}_6$. Since the reported^[16] synthesis of the tetracationic cyclophane, cyclobis(paraquat-*p*-phenylene), employs 1,4-bis[2-(2-hydroxyethoxy)ethoxy]benzene (**16**) (Table 1) as a template, at ultra high pressure (12 kbars) and yields 62% of this cyclophane, the synthesis (Scheme 1) of the cyclophane $4 \cdot 4 \text{ PF}_6$ was attempted^[15] by mixing equimolar amounts of the dicationic salt $15 \cdot 2 \text{ PF}_6$ and the dibromide **13** in the presence of various π -electron-rich templates (Table 1) at both ambient and ultra high (12 kbar) pressures.

At ambient pressure in DMF, whatever the template chosen, formation of the cyclic product was not observed. When the reaction was carried out at high pressure in DMF without a template, only polymeric material was obtained. When either templates **16** or **17** were incorporated^[17] into the reaction mixture, the tetracationic cyclophane $4 \cdot 4 \text{ PF}_6$ was isolated in 5 and 12% yields, respectively.

The self-assembly^[13] of a similar tetracationic cyclophane – namely, cyclobis(paraquat-4,4'-biphenylene) – using ferrocene as a template, suggested an alternative route to us for templating the formation of tetracationic cyclophanes.

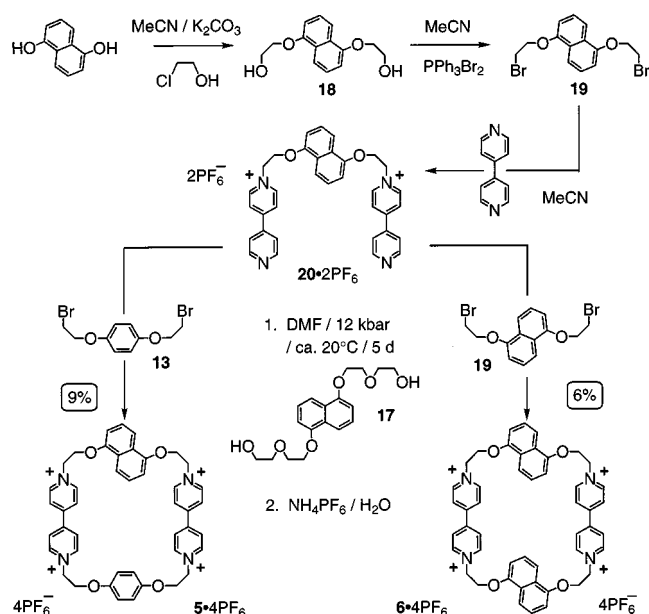
Scheme 1. Template-directed synthesis of the square tetracationic cyclophane $4 \cdot 4 \text{ PF}_6$ Table 1. Yields of formation of the tetracationic cyclophane $4 \cdot 4 \text{ PF}_6$ in different conditions

Template	—			
		Fc	16	17
Yield (%) at 1 bar	0	0	—	0
Yield (%) at 12 kbar	0	0	5	12

Therefore, we decided to use ferrocene as a templating agent for the synthesis of $4 \cdot 4 \text{ PF}_6$, and both surprisingly and unfortunately, we did not observe the formation of the tetracationic cyclophane $4 \cdot 4 \text{ PF}_6$ at either ambient or ultra high pressures.

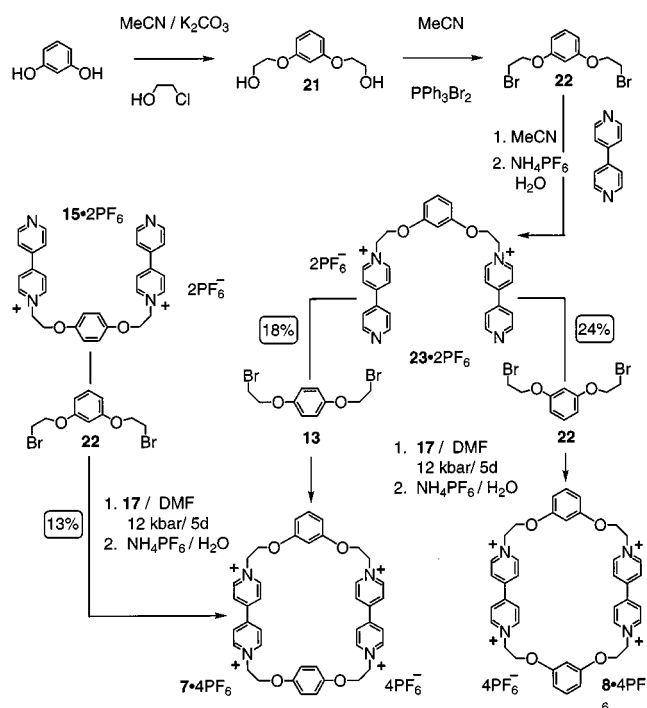
The naphthalene-containing tetracationic cyclophanes $5 \cdot 4 \text{ PF}_6$ and $6 \cdot 4 \text{ PF}_6$ were synthesized, following the synthetic scheme depicted in Scheme 2. The diol **18** was prepared in 56% yield by reaction of 2-chloroethanol with 1,5-naphthalenediol under basic conditions. The dibromide **19** was prepared in 57% yield as a result of reaction of the diol **18** with PPh_3Br_2 in MeCN. Portion-wise addition of the dibromide **19** to a 10-fold excess of 4,4'-bipyridine in MeCN afforded, after counterion exchange, the dicationic salt $20 \cdot 2 \text{ PF}_6$ in 51% yield. Reaction of this salt in turn with the dibromides **13** and **19** in DMF, at 12 kbar, using

1,5-bis[(2-hydroxyethoxy)ethoxy]naphthalene (**17**) as the template afforded, after counterion exchange, the desired tetracationic cyclophanes $5 \cdot 4 \text{ PF}_6$ and $6 \cdot 4 \text{ PF}_6$ in 9 and 6% yields, respectively. These very low yields may be a consequence of the lack of efficiency of the self-assembly process as a consequence of the distorted geometry of the naphthalene spacer unit in $20 \cdot 2 \text{ PF}_6$ with respect to $15 \cdot 2 \text{ PF}_6$ which contains a hydroquinone ring as a spacer.

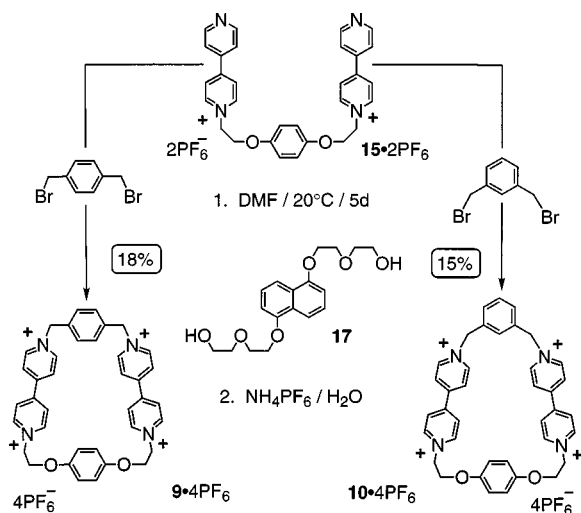
Scheme 2. Template-directed synthesis of the tetracationic cyclophanes 5^{4+} and 6^{4+} 

The synthetic strategy employed in the self-assembly of the tetracationic cyclophanes $7 \cdot 4 \text{ PF}_6$ and $8 \cdot 4 \text{ PF}_6$ relies Scheme 3) upon the same principles as those leading Schemes 1 and 2) to the salts $4-6 \cdot 4 \text{ PF}_6$. Subsequently, the diol **21**, which was prepared in 69% yield from the reaction of 2-chloroethanol with 1,5-naphthalenediol under basic conditions, was treated with PPh_3Br_2 in MeCN to afford the dibromide **22** in 66% yield.

Portion-wise addition of **22** to a 10-fold excess of 4,4'-bipyridine in MeCN afforded, after counterion exchange, the dicationic salt $23 \cdot 2 \text{ PF}_6$ in 62% yield. Reaction of this salt with **22** in DMF using **17** as a template afforded, after counterion exchange, the desired tetracationic cyclophane $8 \cdot 4 \text{ PF}_6$ in 24% yield. The other tetracationic cyclophane $7 \cdot 4 \text{ PF}_6$ was prepared in two different ways – both in the presence of the template **17** – (i) the first way involved the reaction between the dibromide **13** and the dicationic salt $23 \cdot 2 \text{ PF}_6$ and (ii) the second utilized the complementary components – namely the dibromide **22** and the dicationic salt $15 \cdot 2 \text{ PF}_6$. The former method afforded $7 \cdot 4 \text{ PF}_6$ in 18% yield and the latter, $7 \cdot 4 \text{ PF}_6$ in 13% yield. These results may reflect the better preorganization of $23 \cdot 2 \text{ PF}_6$ compared with $15 \cdot 2 \text{ PF}_6$ during the self-assembly process. This hypothesis gains some credence from the fact that, in the solid-state structure of the tetracationic salt $8 \cdot 4 \text{ PF}_6$ (vide infra), the cavity within the macrocycle is narrower than that within $4 \cdot 4 \text{ PF}_6$.

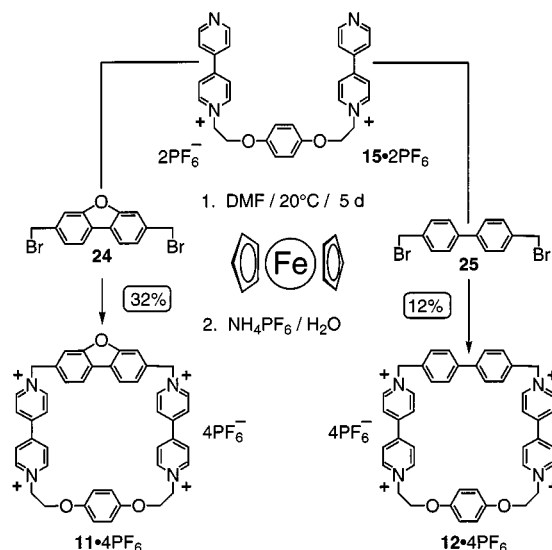
Scheme 3. Template-directed synthesis of the tetracationic cyclophanes 7^{4+} and 8^{4+} 

The tetracationic cyclophanes $9 \cdot 4 \text{ PF}_6$ and $10 \cdot 4 \text{ PF}_6$ were synthesized (Scheme 4) at atmospheric pressure by allowing the dicationic salt $15 \cdot 2 \text{ PF}_6$ to react with dibromo-*p*-xylene and dibromo-*m*-xylene, respectively in MeCN in the presence of the template **17**, giving yields of 18 and 15%.

Scheme 4. Template-directed synthesis of the tetracationic cyclophanes 9^{4+} and 10^{4+} 

The choice of ambient conditions, as opposed to the use of high pressure, relies on the fact that, in this situation, the reactivities of dibromo-*p*-xylene and dibromo-*m*-xylene are much greater than those of the dibromides **13**, **19**, and **22** employed in the previous ring closures.

The tetracationic cyclophanes $11 \cdot 4 \text{ PF}_6$ and $12 \cdot 4 \text{ PF}_6$ were synthesized (Scheme 5) in 12 and 32% yields, respectively, by treating the dicationic salt $15 \cdot 2 \text{ PF}_6$ in turn with the dibromides **24** and **25**, in DMF at ambient pressure in the presence of ferrocene as a template.

Scheme 5. Template-directed synthesis of the tetracationic cyclophanes 11^{4+} and 12^{4+} 

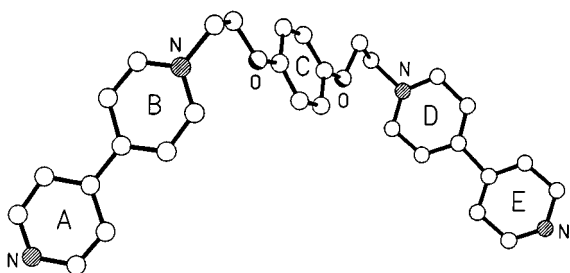
Once again, the benzylic dibromides **24** and **25** are sufficiently reactive to allow the ring closure to occur at atmospheric pressure. By comparison with the results described above, in which ferrocene was shown not to template the ring closure in the synthesis of $4 \cdot 4 \text{ PF}_6$ even at high pressure, here, at normal pressure, a saturated solution of ferrocene enhances the formation of the cyclophanes $11 \cdot 4 \text{ PF}_6$ and $12 \cdot 4 \text{ PF}_6$, resulting in yields of 32 and 12%, respectively.

X-ray Crystallography of $4 \cdot 4 \text{ PF}_6$, $8 \cdot 4 \text{ PF}_6$, and $15 \cdot 2 \text{ PF}_6$

The solid-state structure^[15] of $15 \cdot 2 \text{ PF}_6$ was confirmed by X-ray crystallography. The dicationic salt $15 \cdot 2 \text{ PF}_6$ exhibits (Figure 7) a partially extended skewed horseshoe conformation. The central phenoxymethylene groups are in a *syn* relationship and the $\text{OCH}_2\text{CH}_2\text{N}$ groups adopt *gauche* geometries, both of which are in the same sense. The pyridylpyridinium units are non-planar and exhibit twist angles about the central C–C bond linkages between rings **A** and **B**, and **D** and **E** of 9 and 16°, respectively; there is no noticeable “bowing” of either unit. The skew angle, as defined by the molecular torsional angle $\text{N}(\text{A})-\text{N}(\text{B})/\text{N}(\text{D})-\text{N}(\text{E})$, is 80°.

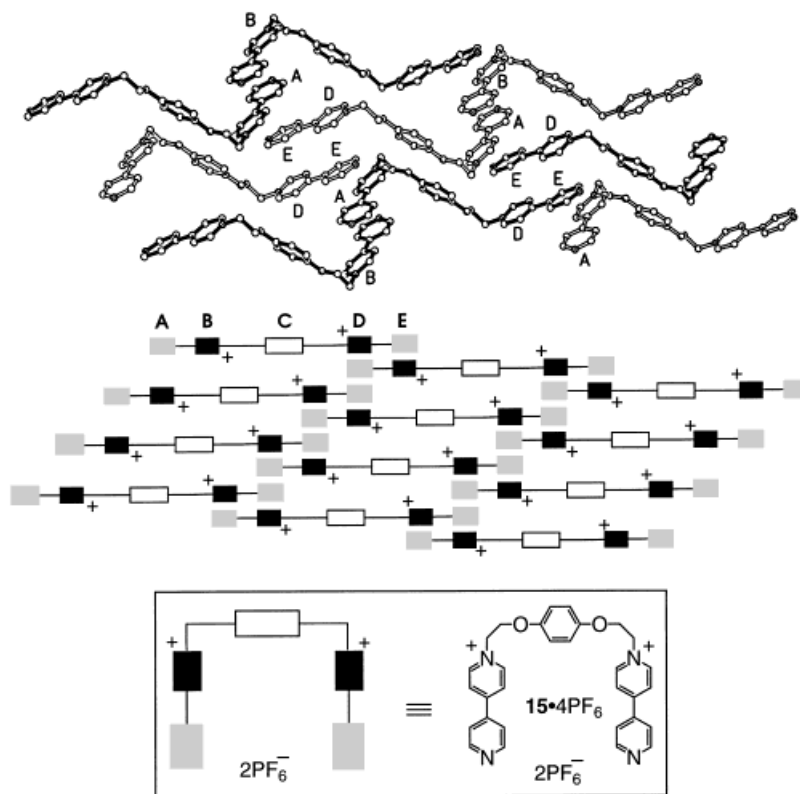
The packing (Figure 8) of the elongated dications is complex, involving extensive intermolecular π - π stacking interactions. The pyridylpyridinium units at each end of the molecule pack in a parallel (**AB**, **BA** and **DE**, **ED**) overlapping relationship with their centrosymmetrically related counterparts creating zig-zag chains (depicted with closed and open bonds, respectively, in Figure 8) that extend in the crystallographic (011) direction. Adjacent chains within the crystal are offset with respect to each other such that the

Figure 7. Ball-and-stick representation of the dicationic salt **15**·2 PF₆ in the solid state



pyridyl ring **A** within one chain is positioned directly above and orthogonally oriented with respect to the pyridyl ring **E** in the next chain. The result of this packing relationship is the formation of extended π - π -stacked sheets (Figure 8) that propagate in the crystallographic *c* direction with a **BAED-DEAB** stepped sequence.

Figure 8. Ball-and-stick (top) and schematic (bottom) representation of the packing in the solid-state structure of the dicationic salt **15**·2 PF₆



In the solid state the tetracationic cyclophane **4**⁴⁺ has (Figure 9) an almost square, open, *C*₂-symmetric geometry, the distances between the corner NCH₂ methylene carbon atoms being 9.88 and 9.94 Å, respectively, the longer distance corresponding to the sides containing the hydroquinone rings. Although these sides of the cyclophane have a planarity that extends to include their adjacent oxybismethylene units, there are quite large twists (20°) between the pyridinium rings in the bipyrindinium units.

The tetracations **4**⁴⁺ pack to form a close-packed two-dimensional π -donor/ π -acceptor mosaic (Figure 9). These

two-dimensional sheets are not planar, there being a slightly stepped relationship between adjacent macrocycles. Despite this terraced arrangement of molecules, there is a retention of a proximal relationship between one of the bipyrindinium rings in one tetracation and a hydroquinone ring in the next and vice versa. The separation between the centroids of these rings in adjacent cyclophanes is 4.0 Å and the planes of the rings are inclined by 22°.

Adjacent sheets, although separated by layers of disordered PF₆⁻ anions and MeCN molecules, are in register and form nanotubes that extend through the crystal. The distance between the cyclophane layers is 9.8 Å, so that two consecutive cyclophanes in adjacent layers form (Figure 10) a cube of ca. 1 nm side.

The X-ray structural analysis of **8**·4 PF₆ reveals (Figure 11) the cyclophane to have a *C*_i-symmetric chair-like conformation, with the resorcinol units inclined by ca. 45° to the mean plane of the macrocycle, and with a ca. 42° twist

between the pyridinium rings within each bipyrindinium unit. The profile of the molecule is rectangular with the distances between the corner NCH₂ methylene carbon atoms of 9.97 and 8.83 Å for the sides incorporating the bipyrindinium units and the resorcinol rings, respectively. The vectors joining these four carbon atoms form a parallelogram with angles of 88 and 92° (angles identical to those observed in **4**⁴⁺).

The molecules pack (Figure 12) head-to-tail with the resorcinol rings in one molecule parallelly π -stacked with those in the next (mean interplanar separation: 3.50 Å, centroid-

Figure 9. Plan view of the packing of 4^{4+} in the solid state (ball-and-stick representation)

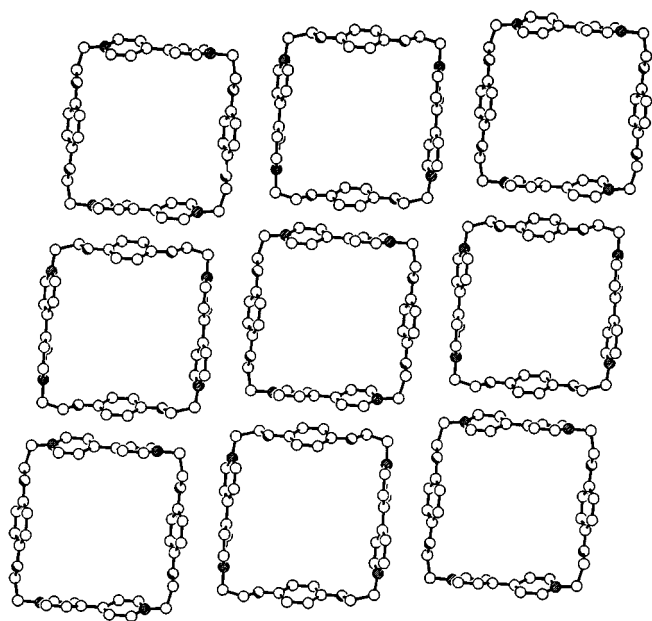
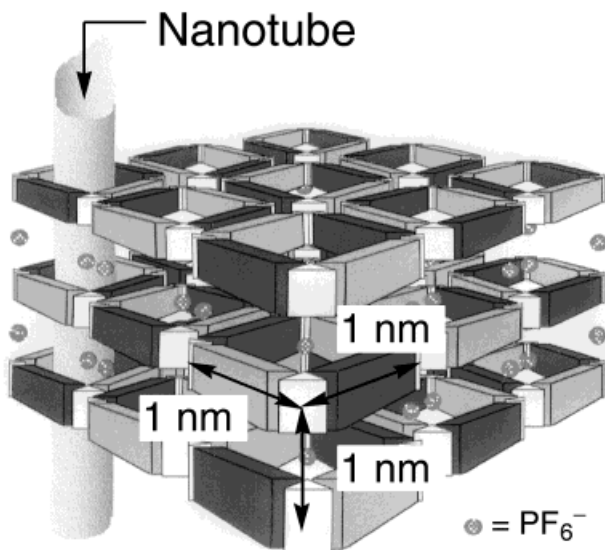


Figure 10. Schematic representation of the channels formed by the tetracations 4^{4+} in the solid state



–centroid distance: 3.64 Å). Adjacent chains in the crystal are oriented orthogonally with respect to each other to form the pseudo close-packed array illustrated in Figure 13. The regions bounded by the confluences of the corners of four adjacent molecules form channels that contain the PF_6^- anions.

Association Constants

The bright green color of a 1:1 molar solution of $4 \cdot 4 \text{ PF}_6$ and ferrocene (**Fc**) in MeCN indicates the formation of a 1:1 adduct $4/\text{Fc} \cdot 4 \text{ PF}_6$ of the inclusion complex type that also displays a charge transfer (CT) interaction.^[19] A UV-spectrophotometric titration, using the CT band centered

Figure 11. Ball-and-stick representation of 8^{4+} in the X-ray structure of $8 \cdot 4 \text{ PF}_6$

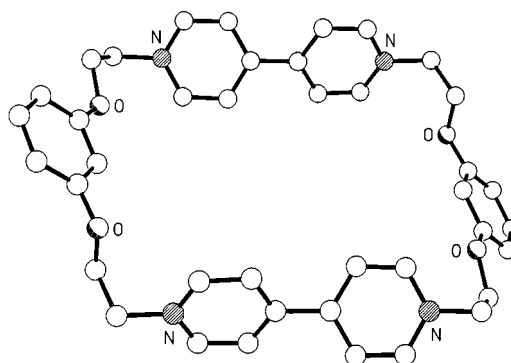


Figure 12. Representation of the packing in the solid-state structure of $8 \cdot 4 \text{ PF}_6$ showing the resorcinol–resorcinol interaction

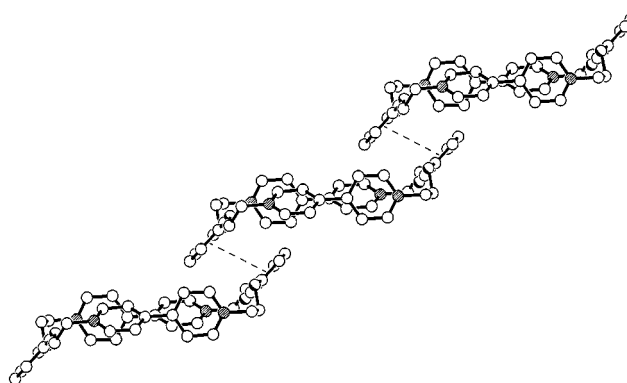
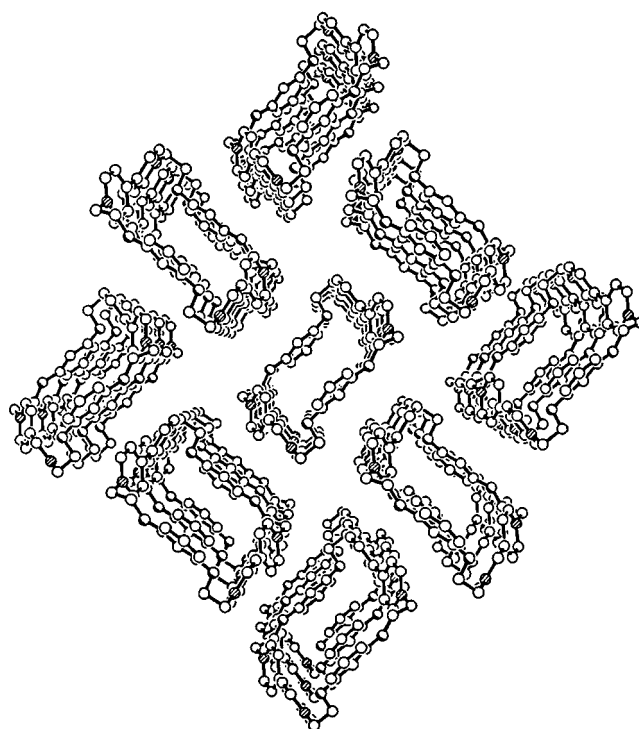
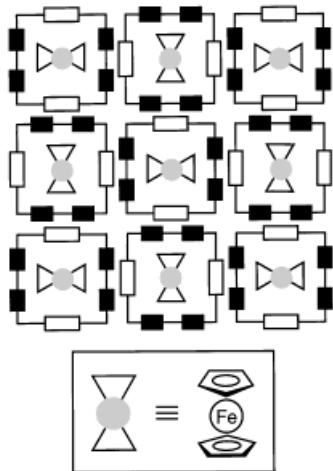


Figure 13. Representation of the packing in the solid-state structure of $8 \cdot 4 \text{ PF}_6$ showing the one-dimensional arrays of π – π -stacked cyclophanes



on 602 nm as the probe, yields an association constant (K_a) of $44 \pm 3 \text{ dm}^3 \text{ mol}^{-1}$ for the 1:1 adduct **4/Fc**·4 PF₆ in MeCN at 25°C. This K_a value corresponds to a free energy of adduct formation of $-2.2 \text{ kcal mol}^{-1}$.

Figure 14. Schematic representation of the anticipated structure of the 1:1 adduct **4/Fc**⁴⁺ in a crystalline state



¹H-NMR-spectroscopic investigations, carried out on a $5.5 \cdot 10^{-3} \text{ M}$ solution of **4/Fc**·4 PF₆ in CD₃CN, indicate that the ferrocene molecule resides within the tetracationic cyclophane with its cyclopentadienyl rings oriented parallel to the planes of the two bipyridinium units in the tetracation. This relative geometry explains the significant upfield shifts (-0.29 ppm) observed for the cyclopentadienyl ring proton resonances of **Fc** and also (-0.08 ppm) for the β -CH bipyridinium signals of **4**⁴⁺. Consequently, it was anticipated that inclusion of ferrocene in this manner should permit the retention (Figure 14) of the mosaic-like array proposed (Figure 3) and observed (Figure 9) in the solid state for **4**·4 PF₆.

All attempts to determine the binding constants between **4**·4 PF₆ and the π -electron-rich guests tetrathiafulvalene (TTF), 1,4-bis[2-(2-hydroxyethoxy)ethoxy]benzene (**16**), 1,5-bis[2-(2-hydroxyethoxy)ethoxy]naphthalene (**17**), and the π -electron-deficient guest tetracyanoquinodimethane (TCNQ) were unsuccessful, as indicated by UV-spectrophotometric or ¹H-NMR-spectrometric titration methods. Although the changes in absorption intensities and chemical shifts were too small to yield any reliable quantitative information, it is obvious from this study that the binding constants must be less than 10 M^{-1} .

The tetracationic cyclophanes **5–12**·4 PF₆ were tested for complexation with ferrocene on its own. The cyclophanes **5–10**·4 PF₆ did not form any stable adducts with ferrocene since no chemical shift changes were observed in the ¹H-NMR spectra of 1:1 mixtures of the two components; also, no charge transfer bands were detected by UV spectrophotometry. When the cyclophanes **11**·4 PF₆ and **12**·4 PF₆ were mixed in a 1:1 ratio with ferrocene, a light green color was observed and could be associated with charge transfer bands centered on 610 and 606 nm, respectively. Once again, however, the absorption changes, moni-

tored by UV spectrophotometry using the titration procedure between ferrocene and **11**·4 PF₆ and **12**·4 PF₆, were far too small to yield any reliable K_a values: again, these binding constants must be less than 10 M^{-1} .

X-ray Crystallography of **4/Fc**·4 PF₆

The X-ray structure^[15] of the C_i-symmetric 1:1 adduct formed between the cyclophane **4**⁴⁺ and ferrocene revealed (Figure 15) the total achievement of the supramolecular design strategy (Figure 14) in that the tetracationic cyclophane includes, via π - π stacking interactions with the bipyridinium units, a ferrocene molecule.^[18] Furthermore, the tetracations self-assemble to form (Figure 16) a π -donor/ π -acceptor two-dimensional mosaic directly analogous to that formed by the free macrocycle. The entrapping of the ferrocene molecule within the tetracationic cyclophane produces only very minor perturbations in its geometry. The lengths of the two sides between the corner NCH₂-carbon atoms are essentially unchanged at 9.83 and 9.95 Å, respectively, and there is only a small reduction, ca. 2°, in the twist angle between the two pyridinium rings of the bipyridinium units. The π - π stacking within the two-dimensional mosaic in the 1:1 adduct is improved with respect to that observed for the free macrocycle. The centroid-centroid separation between the hydroquinone ring in one molecule and one of the pyridinium rings of the next is reduced to 3.8 Å and the rings are closer to parallel, being inclined by only 6° (cf. 22° in **4**⁴⁺). The two-dimensional mosaic sheets are again stacked in register with a mean intersheet separation of 9.8 Å, the PF₆⁻ anions and included solvent molecules being intercalated between the layers.

Conclusion

Consideration of the interactive patterns present in the solid-state structures of 4,4'-bipyridinium-based salts has led us to the design of a series of nine tetracationic cyclophanes **4–12**·4 PF₆ with the potential to form highly ordered arrays of extended π - π -stacked sheets in the solid state. The syntheses of these tetracationic cyclophanes were made possible by carefully tuning the reaction conditions and also by employing, in each case, a template adapted to the target cyclophane. The information present in the molecular structures of the tetracationic cyclophanes **4–12**·4 PF₆ not only facilitated their efficient self-assembly, but also allowed the formation in the solid state of (i) a regular repeating two-dimensional supramolecular array in the case of **4**·4 PF₆, and (ii) linear π - π stacks in the case of **8**·4 PF₆. The solid-state structure of the dicationic salt **15**·2 PF₆ displayed an unusual structure in which pyridylpyridinium units are π - π -interacting with each other in two different ways so as to create two-dimensional π - π stacks. The symmetrically oriented molecular recognition elements of the cyclophane **4**·4 PF₆ have also allowed the directionally specific inclusion of ferrocene (**Fc**) within its cavity to form the 1:1 adduct **4/Fc**·4 PF₆ in both the solid and solution states. We believe that this research should be of relevance to chemists who wish to design novel organic materials with

Figure 15. Ball-and-stick representation of $4/\text{Fe}^{4+}$ in the X-ray structure of $4/\text{Fe} \cdot 4 \text{PF}_6$

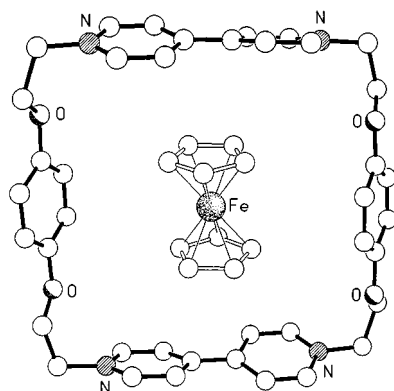
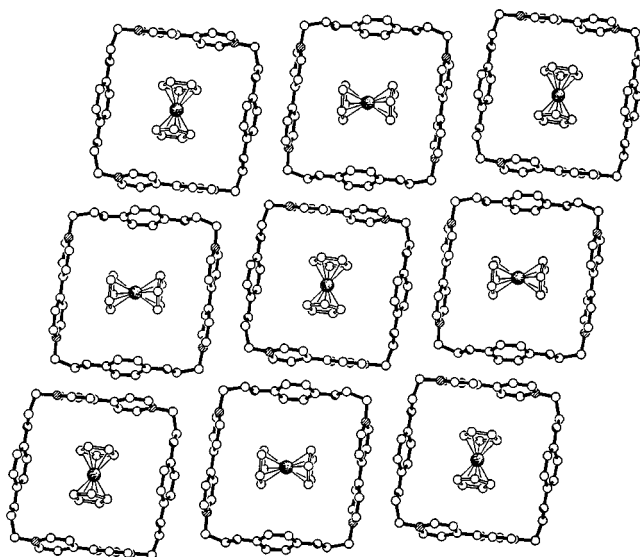


Figure 16. View of the packing of the 1:1 adduct $4/\text{Fe}^{4+}$ in the solid state (ball-and-stick representation)



interesting physical properties, in a way that is reminiscent to the encoding procedure described by the late Margaret Etter^[5b] for hydrogen-bonding interactions.

This research was supported by the *Engineering and Physical Sciences Research Council*, as well as by the *European Community* and by the *Ministère de la Recherche et de l'Enseignement Supérieur* in France. We thank Professor *A. Collet* (Lyon) for helpful discussions. We thank Dr. *M. C. T. Fyfe* and Dr. *M. V. Martinez-Diaz* for providing compounds **24** and **25**, respectively.

Experimental Section

Materials and Methods: Chemicals were purchased from Aldrich and used without further purification. Solvents were either used as purchased or dried (DMF from KOH, MeCN from CaH₂), according to procedures described in the literature.^[20] The reactions requiring ultra high pressure were carried out in a Teflon vessel, using a custom-built reactor, manufactured by PSIKA Pressure Systems Limited of Glossop in the UK. – Thin-layer chromatography (TLC) was carried out using aluminum sheets precoated with silica gel 60F (Merck 5554). The plates were inspected by UV light and developed with a dilute solution of I₂ in CHCl₃. – Column chro-

matography was carried out using silica gel 60F (Merck 9385, 230–400 mesh). – Melting points were determined with an Electrothermal 9200 apparatus and are not corrected. – Low-resolution mass spectra were performed using a Kratos Profile spectrometer, operating in electron impact (EIMS) mode. Fast-atom bombardment mass spectra (FABMS) were recorded with a Kratos MS80 spectrometer operating at 8 keV using a xenon primary atom beam. The matrix used was 3-nitrobenzyl alcohol (NOBA). Liquid Secondary Ion Mass Spectra (LSIMS) were recorded with a VG ZabSpec mass spectrometer, using an *m*-nitrobenzyl alcohol matrix and a scan speed of 10 s per decade.

Tetracationic Cyclophane $4 \cdot 4 \text{PF}_6$: The dibromide **13** (32.4 mg, 0.1 mmol), the dicationic salt **15** $\cdot 2 \text{PF}_6$ (76.6 mg, 0.1 mmol), and the diol **17** (100.9 mg, 0.3 mmol) were dissolved in dry DMF (10 ml). The reaction mixture was transferred to a high-pressure reaction Teflon tube, which was then compressed (12 kbars) at room temperature for 5 d. The precipitate, which resulted on addition of Et₂O (150 ml), was filtered off and purified by column chromatography [SiO₂; MeOH/2 N aqueous NH₄Cl/MeNO₂ (7:2:1)] to yield, after counterion exchange, $4 \cdot 4 \text{PF}_6$ as a deep yellow solid (15 mg, 12%); m.p. > 260 °C. – FABMS; *m/z*: 1075 [M – PF₆]⁺. – ¹H NMR (300 MHz, CD₃CN, 25 °C): δ = 8.94 (d, 8 H), 8.36 (d, 8 H), 6.71 (s, 8 H), 4.98 (t, 8 H), 4.31 (t, 8 H). – ¹³C NMR (75.5 MHz, CD₃CN, 25 °C): δ = 153.5, 150.8, 147.3, 127.6, 116.3, 67.5, 62.3. – HRLSIMS: calcd. for C₄₀H₄₀F₁₂N₄O₄P₂ [M – 2 PF₆]⁺; *m/z* 930.2333; found: *m/z* 930.2375. – Single crystals, suitable for X-ray crystallography, were grown by vapor diffusion of *i*Pr₂O into a solution of $4 \cdot 4 \text{PF}_6$ in MeCN.

1,5-Bis(2-hydroxyethoxy)naphthalene (18**):** 2-Chloroethanol (8.68 g, 108 mmol) was added during 1 h to a refluxing solution of 1,5-naphthalenediol (5.76 g, 36 mmol) and K₂CO₃ (30 g, 217.7 mmol) in MeCN (200 ml) under N₂. The reaction mixture was kept under reflux for 48 h and filtered. The filtrate was concentrated and the residue was dissolved in CH₂Cl₂ (100 ml). The solution was washed with H₂O (2 \times 30 ml) and brine (30 ml), dried (MgSO₄), concentrated in vacuo, and the resulting dark brown residue was extracted with hot EtOAc (5 \times 50 ml). The solution was then concentrated in vacuo and the brown residue was crystallized from Me₂CO to yield the diol **18** as a brown solid (5.0 g, 56%); m.p. 180–181 °C. – EIMS; *m/z*: 248 [M]⁺. – ¹H NMR (300 MHz, CD₃CN, 25 °C): δ = 7.81 (d, *J* = 8.5 Hz, 2 H), 7.38 (t, *J* = 8.0 Hz, 2 H), 6.98 (d, *J* = 8.0 Hz, 2 H), 4.99 (t, *J* = 5.0 Hz, 2 H), 4.14 (t, *J* = 5.0 Hz, 4 H), 3.87–3.83 (m, 4 H). – ¹³C NMR (CD₃CN, 75 MHz, 25 °C): δ = 154.1, 126.1, 125.3, 114.0, 105.8, 70.0, 59.8.

1,5-Bis(2-bromoethoxy)naphthalene (19**):** Br₂ (2.28 g, 8.0 mmol) was added to a mechanically stirred suspension of Ph₃P (2.11 g, 8.0 mmol) in dry MeCN (100 ml) at 5 °C at such a rate that the supernatant solution remained colorless. The solution was then allowed to warm up to room temperature and powdered 1,5-bis(2-hydroxyethoxy)naphthalene (1.00 g, 4.0 mmol) was added in one portion. After 48 h, the precipitate which formed was collected and crystallized from MeOH to obtain the dibromide **19** as a beige solid (850 mg, 57%); m.p. 146 °C. – EIMS; *m/z*: 374 [M]⁺. – ¹H NMR (300 MHz, CD₃CN, 25 °C): δ = 7.87 (d, *J* = 8.0 Hz, 2 H), 7.41 (t, *J* = 7.7 Hz, 2 H), 6.95 (d, *J* = 7.7 Hz, 2 H), 4.47 (t, *J* = 5.5 Hz, 4 H), 3.85 (t, *J* = 5.5 Hz, 4 H). – ¹³C NMR (CD₃CN, 75 MHz, 25 °C): δ = 154.3, 126.2, 125.2, 114.8, 105.7, 69.1, 31.6.

Dicationic Salt $20 \cdot 2 \text{PF}_6$: The dibromide **19** (0.50 g, 1.3 mmol) was added portion-wise during 7 d, three times per d (24 mg per portion), to a refluxing solution of 4,4'-bipyridine (2.09 g, 13.4 mmol) in dry MeCN (50 ml) under nitrogen. The reaction mixture was maintained under reflux for a further 48 h before it was al-

lowed to cool down to room temperature, whereupon the brown precipitate was filtered and dissolved in a mixture of Me₂CO and H₂O, before being purified by column chromatography [SiO₂; MeOH/2 N aqueous NH₄Cl/MeNO₂ (7:2:1)] to yield, after counterion exchange, the dicationic salt **20**·2 PF₆ as a yellow-green solid (556 mg, 51%); m.p. > 240°C. – FABMS; *m/z*: 671 [M – PF₆]⁺. – ¹H NMR (300 MHz, CD₃CN, 25°C): δ = 8.95 (d, *J* = 7.0 Hz, 4 H), 8.81 (d, *J* = 7.0 Hz, 4 H), 8.34 (d, *J* = 7.0 Hz, 4 H), 7.76–7.71 (m, 6 H), 7.40 (t, 7.7 Hz, 2 H), 6.96 (d, *J* = 7.35 Hz, 2 H), 5.07 (t, *J* = 4.8 Hz, 4 H), 4.62 (t, *J* = 4.8 Hz, 4 H). – ¹³C NMR (CD₃CN, 75 MHz, 25°C): δ = 155.5, 153.9, 151.9, 146.4, 141.9, 126.7, 126.5, 122.6, 118.5, 115.6, 67.2, 61.4.

1,3-Bis(2-hydroxyethoxy)benzene (21): A solution of resorcinol (5 g, 45.4 mmol) in EtOH (70 ml) was added dropwise over 15 min to a stirred solution of NaOH (5.44 g, 136.2 mmol) in EtOH (70 ml) and H₂O (24 ml). A solution of 2-chloroethanol (11.00 g, 136.2 mmol) in EtOH (70 ml) was then added dropwise over 20 min and the reaction mixture was heated under reflux for 3 d. After cooling down to room temperature, the reaction mixture was filtered to afford the diol **21** as a white solid (2.0 g). The mother liquor was then concentrated in vacuo to leave a yellow oil which was partitioned between CH₂Cl₂ (150 ml) and brine (70 ml). The pH of the aqueous layer was adjusted to ca. 2 using 2 N HCl. The aqueous layer was extracted with CH₂Cl₂ (4 × 50 ml) and the combined organic layers were concentrated in vacuo to afford the diol **21** as a white solid (2.2 g, 4.2 g overall, 69%); m.p. 97°C. – EIMS; *m/z*: 198 [M]⁺. – ¹H NMR (300 MHz, CD₃COCD₃, 25°C): δ = 7.18–7.12 (1 H, m), 6.55–6.50 (3 H, m), 4.08–4.00 (4 H, m), 3.95 (2 H, t, *J* = 5.0 Hz), 3.88–3.80 (4 H, m). – ¹³C NMR (CD₃COCD₃, 75 MHz, 25°C): δ = 161.2, 130.6, 107.5, 102.1, 70.3, 61.3.

1,3-Bis(2-bromoethoxy)benzene (22): Br₂ (1.3 ml, 25.2 mmol) was added dropwise to a vigorously stirred suspension of Ph₃P (6.62 g, 25.2 mmol) in dry MeCN (25 ml). The reaction mixture was maintained at < 5°C during the addition and then allowed to warm up to room temperature before the diol **21** (2.5 g, 12.6 mmol) was added to it in one portion. The reaction mixture was stirred for 4 h at room temperature, after which time it was filtered, and the solvent removed under vacuum, giving a white solid which was crystallized from MeOH to afford the dibromide **22** as a white solid (2.7 g, 66%); m.p. 87°C. – EIMS; *m/z*: 324 [M]⁺. – ¹H NMR (300 MHz, CD₃CN, 25°C): δ = 7.22 (t, *J* = 7.5 Hz, 1 H), 6.57 (dd, *J* = 7.5 Hz, 2 H), 6.50 (t, *J* = 2.5 Hz, 1 H), 4.30 (t, *J* = 5.5 Hz, 4 H), 3.70 (t, *J* = 5.5 Hz, 4 H). – ¹³C NMR (CD₃CN, 75 MHz, 25°C): δ = 160.8, 131.5, 108.8, 102.9, 69.3, 31.6.

Dicationic Salt 23·2 PF₆: The dibromide **22** (1.05 g, 3.24 mmol) was added portion-wise every 8 h over 7 d to a refluxing solution of 4,4'-bipyridine (5.05 g, 3.24 mmol) in dry MeCN (100 ml). The reaction mixture was maintained under reflux for a further 48 h. Then, it was allowed to cool down to room temperature, whereupon the greenish-brown precipitate which formed was filtered off and dissolved in H₂O before being purified by column chromatography [SiO₂; MeOH/2 N aqueous NH₄Cl/MeNO₂ (7:2:1)]. The fractions containing the product were combined and concentrated under vacuum to give a residue which was dissolved in H₂O. The dicationic salt **23**·2 PF₆ was precipitated from this solution by addition of a saturated aqueous NH₄PF₆ solution. The dication was isolated as a beige solid (1.55 g, 62%); m.p. > 215°C. – FABMS; *m/z*: 621 [M – PF₆]⁺. – ¹H NMR (300 MHz, CD₃COCD₃, 25°C): δ = 9.35 (d, *J* = 7.5 Hz, 4 H), 8.87 (d, *J* = 7.5 Hz, 4 H), 8.68 (d, *J* = 7.5 Hz, 4 H), 8.00 (d, *J* = 5 Hz, 4 H), 7.19 (t, *J* = 7.5 Hz, 1 H), 6.69–6.57 (m, 3 H), 5.30 (t, *J* = 5 Hz, 4 H), 4.67 (t, *J* = 5 Hz,

4 H). – ¹³C NMR (CD₃COCD₃, 75 MHz, 25°C): δ = 159.9, 155.4, 152.2, 147.1, 142.0, 131.2, 126.7, 122.8, 108.6, 102.9, 67.2, 61.7.

General Procedure for the Syntheses of the Tetracationic Cyclophanes 5–8·4 PF₆: The dibromide (0.1 mmol), the dicationic salt (0.1 mmol), and the diol **17** (100.9 mg, 0.3 mmol) were dissolved in dry DMF (10 ml). The reaction mixture was transferred to a high-pressure reaction Teflon tube, which was then compressed (12 kbars) at room temperature for 5 d. The precipitate, which resulted on addition of Et₂O (150 ml), was filtered off and purified by column chromatography [SiO₂; MeOH/2 N aqueous NH₄Cl/MeNO₂ (7:2:1)] to yield, after counterion exchange, the desired tetracationic cyclophane.

Tetracationic Cyclophane 5·4 PF₆: Yield 9%; m.p. > 260°C. – FABMS; *m/z*: 1125 [M – PF₆]⁺. – ¹H NMR (300 MHz, CD₃CN, 25°C): δ = 9.05 (d, *J* = 7.0 Hz, 4 H), 8.88 (d, *J* = 7.0 Hz, 4 H), 8.35 (d, *J* = 7.0 Hz, 4 H), 8.30 (d, *J* = 7.0 Hz, 4 H), 7.86 (d, *J* = 8.4 Hz, 2 H), 7.37 (t, *J* = 7.7 Hz, 2 H), 6.82 (d, *J* = 7.7 Hz, 2 H), 6.64 (s, 4 H), 5.17 (t, *J* = 4.4 Hz, 4 H), 4.93 (t, *J* = 4.4 Hz, 4 H), 4.59 (t, *J* = 4.4 Hz, 4 H), 4.26 (t, *J* = 4.4 Hz, 4 H). – ¹³C NMR (CD₃CN, 75 MHz, 25°C): δ = 153.4, 151.0, 147.3, 146.3, 145.0, 127.9, 127.6, 126.7, 116.5, 115.9, 107.2, 67.7, 67.5, 62.2. – HRLSIMS: calcd. for C₄₄H₄₂F₁₂N₄O₄P₂ [M – 2 PF₆]⁺: *m/z* 980.2490; found: *m/z* 980.2487.

Tetracationic Cyclophane 6·4 PF₆: Yield 6%; m.p. > 260°C. – FABMS; *m/z*: 1175 [M – PF₆]⁺. – ¹H NMR (300 MHz, CD₃CN, 25°C): δ = 9.01 (d, *J* = 7.0 Hz, 8 H), 8.30 (d, *J* = 7.0 Hz, 8 H), 7.77 (d, *J* = 8.4 Hz, 4 H), 7.32 (t, *J* = 7.7 Hz, 4 H), 6.78 (d, *J* = 7.7 Hz, 4 H), 5.14 (t, *J* = 4.4 Hz, 8 H), 4.52 (t, *J* = 4.4 Hz, 8 H). – ¹³C NMR (CD₃CN, 75 MHz, 25°C): δ = 154.0, 150.6, 147.2, 126.9, 126.7, 115.6, 106.8, 67.7, 62.4. – C₄₈H₄₄F₂₄N₄O₄P₄ (1320.8): calcd. C 43.65, H 3.36, N 4.24; found C 43.60, H 3.39, N 4.26.

Tetracationic Cyclophane 7·4 PF₆: Yield 13% from **15**·2 PF₆ and **22**, 18% from **13** and **23**·2 PF₆; m.p. > 225°C. – FABMS; *m/z*: 1075 [M – PF₆]⁺. – ¹H NMR (CD₃CN, 300 MHz, 25°C): δ = 8.95 (d, *J* = 6.2 Hz, 4 H), 8.91 (d, *J* = 6.2 Hz, 4 H), 8.34–8.25 (m, 8 H), 7.23 (t, *J* = 8.5, 1 H), 6.72 (s, 4 H), 6.61–6.54 (m, 2 H), 6.49 (s, 1 H), 4.99–4.92 (m, 8 H), 4.44–4.37 (m, 4 H), 4.36–4.29 (m, 4 H). – ¹³C NMR (CD₃CN, 75 MHz, 25°C): δ = 159.6, 153.3, 151.2, 147.1, 131.3, 127.8, 127.7, 116.2, 107.1, 104.1, 67.5, 66.7, 62.2. – HRLSIMS: calcd. for C₄₀H₄₀F₁₂N₄O₄P₂ [M – 2 PF₆]⁺: *m/z* 930.2333; found: *m/z* 930.2333.

Tetracationic Cyclophane 8·4 PF₆: Yield 24%; m.p. > 230°C. – FABMS; *m/z*: 1075 [M – PF₆]⁺. – ¹H NMR (300 MHz, CD₃CN, 25°C): δ = 8.99 (d, *J* = 7.0 Hz, 8 H), 8.38 (d, *J* = 7.0 Hz, 8 H), 7.23 (t, *J* = 8.45 Hz, 2 H), 6.60–6.50 (m, 6 H), 5.00 (t, *J* = 4.4 Hz, 8 H), 4.42 (t, *J* = 4.4 Hz, 8 H). – ¹³C NMR (CD₃CN, 75 MHz, 25°C): δ = 159.7, 151.2, 147.3, 131.6, 127.9, 107.2, 104.9, 66.7, 62.2. – C₄₀H₄₀F₂₄N₄O₄P₄ (1220.6): calcd. C 39.36, H 3.30, N 4.59; found C 39.12, H 3.18, N 4.63. – Single crystals, suitable for X-ray crystallography, were grown by vapor diffusion of *i*Pr₂O into a solution of **8**·4 PF₆ in MeCN.

General Procedure for the Syntheses of the Cyclophanes 9–10·4 PF₆: The dibromide (0.1 mmol), the dicationic salt (0.1 mmol), and the diol **17** (100.9 mg, 0.3 mmol) were dissolved in dry MeCN (10 ml). The reaction mixture was stirred at room temperature for 14 d and then concentrated in vacuo. The residue was purified by column chromatography [SiO₂; MeOH/2 N aqueous NH₄Cl/MeNO₂ (7:2:1)] to yield, after counterion exchange, the desired tetracationic cyclophane.

Tetracationic Cyclophane 9·4 PF₆: Yield 18%; m.p. > 230°C. – FABMS; *m/z*: 1015 [M – PF₆]⁺. – ¹H NMR (300 MHz, CD₃CN,

25°C): δ = 8.91–8.87 (m, 8 H), 8.28–8.24 (m, 8 H), 7.58 (s, 4 H), 6.58 (s, 4 H), 5.78 (s, 4 H), 4.93 (d, J = 4.4 Hz, 4 H), 4.24 (d, J = 4.8 Hz, 4 H). – ^{13}C NMR (75 MHz, CD_3CN , 25°C): δ = 153.5, 150.6, 150.5, 147.1, 146.2, 136.0, 131.3, 128.1, 127.4, 116.3, 68.0, 65.3, 62.1. – HRMSIMS: calcd. for $\text{C}_{38}\text{H}_{36}\text{F}_{12}\text{N}_4\text{O}_2\text{P}_2$ [$\text{M} - 2\text{PF}_6$] $^+$: m/z 870.2122; found: m/z 870.2107.

Tetracationic Cyclophane 10·4 PF_6 : Yield 15%; m.p. > 225°C. – FABMS; m/z : 1015 [$\text{M} - \text{PF}_6$] $^+$. – ^1H NMR (300 MHz, CD_3CN , 25°C): δ = 8.90 (d, J = 7 Hz, 4 H), 8.82 (d, J = 7.0 Hz, 4 H), 8.27 (d, J = 7 Hz, 4 H), 8.22 (d, J = 7.0 Hz, 4 H), 7.57–7.84 (m, 4 H), 6.61 (s, 4 H), 5.78 (s, 4 H), 4.93 (t, J = 4.8 Hz, 4 H), 4.29 (t, J = 4.8 Hz, 4 H). – ^{13}C NMR (75 MHz, CD_3CN , 25°C): δ = 153.7, 151.0, 147.3, 146.1, 134.4, 133.5, 132.0, 131.9, 128.0, 127.5, 116.3, 68.2, 65.0, 62.4. – HRMSIMS: calcd. for $\text{C}_{38}\text{H}_{36}\text{F}_{12}\text{N}_4\text{O}_2\text{P}_2$ [$\text{M} - 2\text{PF}_6$] $^+$: m/z 870.2122; found: m/z 870.2101.

General Procedure for the Syntheses of the Cyclophanes 11–12·4 PF_6 : The dibromide (0.1 mmol), the dicationic salt (0.1 mmol), and ferrocene (409 mg, 2.2 mmol) were dissolved in dry MeCN (10 ml). The reaction mixture was stirred at room temperature for 14 d and then concentrated in vacuo. The residue was purified by column chromatography [SiO_2 ; MeOH/2 N aqueous $\text{NH}_4\text{Cl}/\text{MeNO}_2$ (7:2:1)] to yield, after counterion exchange, the desired tetracationic cyclophane.

Tetracationic Cyclophane 11·4 PF_6 : Yield 32%; m.p. > 250°C. – FABMS; m/z : 1105 [$\text{M} - \text{PF}_6$] $^+$. – ^1H NMR (300 MHz, CD_3CN , 25°C): δ = 8.95–8.90 (m, 8 H), 8.31–8.28 (m, 8 H), 8.17 (d, J = 8.1 Hz, 2 H), 7.69 (d, J = 8.1 Hz, 2 H), 7.39 (s, 2 H), 6.68 (s, 4 H), 5.96 (s, 4 H), 4.96 (t, J = 5.0 Hz, 4 H), 4.26 (t, J = 5.0 Hz, 4 H). – ^{13}C NMR (75 MHz, CD_3CN , 25°C): δ = 157.9, 153.3, 150.9, 150.8, 147.2, 146.6, 135.2, 128.4, 127.7, 125.7, 123.5, 116.0, 112.6, 67.2, 66.0, 62.2. – $\text{C}_{44}\text{H}_{38}\text{F}_{24}\text{N}_4\text{O}_3\text{P}_4$ (1250.7): calcd. C 42.26, H 3.06, N 4.48; found C 41.95, H 3.08, N 4.34.

Tetracationic Cyclophane 12·4 PF_6 : Yield 12%; m.p. > 245°C. – FABMS; m/z : 1091 [$\text{M} - \text{PF}_6$] $^+$. – ^1H NMR (300 MHz, CD_3CN , 25°C): δ = 8.94–8.87 (m, 8 H), 8.29–8.25 (m, 8 H), 6.65 (s, 4 H), 5.80 (s, 4 H), 4.94–4.91 (m, 4 H), 4.25–4.22 (m, 4 H). – ^{13}C NMR (75 MHz, CD_3CN , 25°C): δ = 157.7, 150.8, 147.2, 146.3, 15.3, 130.8, 128.9, 128.5, 127.7, 116.0, 67.1, 66.1, 62.2. – HRMSIMS: calcd. for $\text{C}_{44}\text{H}_{40}\text{F}_{12}\text{N}_4\text{O}_2\text{P}_2$ [$\text{M} - 2\text{PF}_6$] $^+$: m/z 946.2435; found: m/z 946.2415.

The 1:1 Adduct 4/Fc·4 PF_6 : For the 1:1 adduct ($5.5 \cdot 10^{-3}$ M): ^1H NMR (300 MHz, CD_3CN , 25°C): δ = 8.89 (d, 8 H), 8.28 (d, 8 H), 6.74 (s, 8 H), 4.96 (t, 8 H), 4.31 (t, 8 H), 3.87 (s, 10 H). – Single crystals, suitable for X-ray crystallography, were grown by vapor diffusion of $i\text{Pr}_2\text{O}$ into a 1:1 solution of 4·4 PF_6 and ferrocene (Fc) in MeCN.

X-ray Crystallography: The data for all compounds with the exception of 8·4 PF_6 have already been deposited. Table 2 provides a summary of the crystal data, data collection, and refinement parameters for 8·4 PF_6 , and for comparison those for 15·2 PF_6 , 4·4 PF_6 , and 4/Fc·4 PF_6 .^[15] The structure of 8·4 PF_6 was solved by direct methods and the non-hydrogen atoms refined anisotropically. There was evidence for disorder in the PF_6^- anions but this could not be resolved into alternate partial occupancy orientations. The positions of the hydrogen atoms were idealized, assigned as isotropic thermal parameters $U(\text{H}) = 1.2U_{\text{eq}}(\text{C})$, and allowed to ride on their parent carbon atoms. Refinement was by full-matrix least squares based on F^2 . Computations were carried out using the SHELXTL program system (version 5.03). The crystallographic data (excluding structure factors) for the structure reported in this paper have been deposited with the Cambridge Crystallographic Data Centre as supplementary publication no. CCDC-101398. Copies of the data can be obtained free of charge on application to

Table 2. Crystal data, data collection, and refinement parameters for 15·2 PF_6 , 4·4 PF_6 , 8·4 PF_6 , and 4/Fc·4 PF_6 ^[a]

Data	15·2 PF_6	4·4 PF_6 ^[b]	8·4 PF_6 ^[b]	4/Fc·4 PF_6 ^[b]
Empirical formula	$\text{C}_{30}\text{H}_{30}\text{N}_4\text{O} \cdot 2\text{PF}_6$	$\text{C}_{40}\text{H}_{40}\text{N}_4\text{O}_4 \cdot 4\text{PF}_6$	$\text{C}_{40}\text{H}_{40}\text{N}_4\text{O}_4 \cdot 4\text{PF}_6$	$\text{C}_{50}\text{H}_{50}\text{FeN}_4\text{O}_4 \cdot 4\text{PF}_6$
Solvent	0.5 H_2O	2.3 MeCN	—	2 MeCN/2 H_2O
M	777.5	1315.1	1220.6	1524.8
Colour, habit	clear prisms	yellow blocks	clear prisms	green blocks
Crystal size [mm]	0.67×0.63×0.50	0.23×0.27×0.33	0.17×0.17×0.10	0.20×0.20×0.23
Crystal system	triclinic	monoclinic	monoclinic	monoclinic
Space group	$P1$	C_2/c	$P2_1/n$	$P2_1/c$
Temperature [K]	291	293	203	293
a [Å]	10.459(7)	22.990(7)	11.308(1)	9.834(2)
b [Å]	11.811(8)	20.372(6)	13.902(1)	20.450(4)
c [Å]	14.522(12)	17.476(5)	15.265(1)	16.767(3)
α [°]	92.56(2)	—	—	—
β [°]	110.81(2)	124.00(2)	92.95(4)	103.09(2)
γ [°]	90.67(2)	—	—	—
V [Å ³]	1675(2)	6785(4)	2396.4(3)	3284(1)
Z	2	4 ^[c]	2 ^[c]	2 ^[c]
D_c [g cm ^{−3}]	1.542	1.287	1.692	1.542
$F(000)$	794	2666.4	2820	1552
μ [mm ^{−1}]	2.14	1.99	1.47	3.85
2 θ range [°]	3.0–110.0	3.0–110.0	8.6–110.0	3.0–120.0
Independent reflections	4216	4268	2995	4860
Observed reflections, $ F_o > 4\sigma(F_o)$	2411	2512	2430	2348
Number of parameters	509	444	343	425
R_1 ^[d]	0.138 ^[e]	0.118 ^[e]	0.090 ^[f]	0.118 ^[e]
R_w ^[g]	0.157	0.127	0.2352 ^[h]	0.116
Largest difference peak, hole [eÅ ^{−3}]	0.53, −0.37	0.55, −0.38	0.69, −0.66	0.60, −0.49

^[a] Details in common: graphite-monochromated Cu- K_α radiation, ω -scans Siemens PA diffractometer). – ^[b] Rotating anode source. – ^[c] The molecule has crystallographic C_2 symmetry. – ^[d] $R_1 = \sum ||F_o| - |F_c|| / \sum |F_o|$. – ^[e] Refinement based on F . – ^[f] Refinement based on F^2 . – ^[g] $R_w = \sum (|F_o| - |F_c|)w^{1/2} / \sum |F_o|w^{1/2}$, $w^{-1} = \sigma^2(F) + 0.00050 F^2$. – ^[h] Value quoted is for $wR_2 = [\sum w(F_o^2 - F_c^2)^2 / \sum w(F_o^2)^2]^{1/2}$, $w^{-1} = \sigma^2(F_o^2) + (0.134 P)^2 + 9.500 P$.

CCDC, 12 Union Road, Cambridge CB2 1EZ, UK [fax: int. code +44(0)1223/336-033; e-mail: deposit@ccdc.cam.ac.uk].

- [1] [1a] J. S. Lindsey, *New. J. Chem.* **1991**, 15, 153–180. — [1b] G. M. Whitesides, J. P. Mathias, C. T. Seto, *Science* **1991**, 254, 1312–1319. — [1c] G. M. Whitesides, E. R. Simanek, J. P. Mathias, C. T. Seto, D. N. Chin, M. Mammen, D. M. Gordon, *Acc. Chem. Res.* **1995**, 28, 37–44. — [1d] D. S. Lawrence, T. Jiang, M. Levett, *J. Am. Chem. Soc.* **1995**, 95, 2229–2260. — [1e] D. Philp, J. F. Stoddart, *Synlett* **1991**, 445–458. — [1f] D. Philp, J. F. Stoddart, *Angew. Chem. Int. Ed. Engl.* **1996**, 35, 1154–1196; *Angew. Chem.* **1996**, 108, 1242–1286.
- [2] [2a] H. M. Colquhoun, J. F. Stoddart, D. J. Williams, *J. Chem. Soc., Chem. Commun.* **1981**, 847–849; H. M. Colquhoun, D. F. Lewis, J. F. Stoddart, D. J. Williams, *J. Chem. Soc. Dalton Trans.* **1983**, 607–613. — [2b] Y.-L. Chang, M.-A. West, F. W. Fowler, J. W. Lauher, *J. Am. Chem. Soc.* **1993**, 115, 5991–6000. — [2c] J. C. MacDonald, G. M. Whitesides, *Chem. Rev.* **1994**, 94, 2383–2420. — [2d] M. Kotera, J.-M. Lehn, J.-P. Vigneron, *J. Chem. Soc., Chem. Commun.* **1994**, 197–199; J. Yang, J.-L. Marendaz, S. J. Geib, A. D. Hamilton, *Tetrahedron Lett.* **1994**, 35, 3665–3668. — [2e] J. C. Besson, L. J. Fitzgerald, J. C. Gallucci, R. E. Gerkin, J. T. Rademacher, A. W. Czarnik, *J. Am. Chem. Soc.* **1994**, 116, 4621–4622. — [2f] A. Houlton, D. Michael, P. Mingos, D. J. Williams, *J. Chem. Soc., Chem. Commun.* **1994**, 503–504. — [2g] P. R. Ashton, C. L. Brown, S. Menzer, S. A. Nepogodiev, J. F. Stoddart, D. J. Williams, *Chem. Eur. J.* **1996**, 2, 580–591. — [2h] K. Eichhorst-Gerner, A. Stabel, G. Moessner, D. Declercq, S. Valiyveetil, V. Enkelmann, K. Müllen, J. P. Rabe, *Angew. Chem. Int. Ed. Engl.* **1996**, 35, 1492–1495; *Angew. Chem.* **1996**, 108, 1599–1602. — [2i] R. F. M. Lange, F. H. Beijer, R. P. Sijbesma, R. W. W. Hooft, H. Kooijman, A. L. Spek, J. Kroon, E. W. Meijer, *Angew. Chem. Int. Ed. Engl.* **1997**, 36, 969–971; *Angew. Chem.* **1997**, 109, 1006–1008.
- [3] [3a] Y. S. Obeng, M. E. Laing, A. C. Friedli, H. C. Yang, D. Wang, E. W. Thulstrup, A. J. Bard, J. Michl, *J. Am. Chem. Soc.* **1992**, 114, 9943–9952. — [3b] H. O. Stumpf, L. Ouahab, Y. Pei, D. Grandjean, O. Kahn, *Science* **1993**, 260, 1762–1763. — [3c] M. Munakata, T. Kuroda-Sowa, M. Maekawa, M. Nakamura, S. Akiyama, S. Kitagawa, *Inorg. Chem.* **1994**, 33, 1284–1291. — [3d] S. Kawata, S. Kitagawa, M. Kondo, I. Furuchi, M. Munakata, *Angew. Chem. Int. Ed. Engl.* **1994**, 33, 1759–1761; *Angew. Chem.* **1994**, 106, 1851–1854. — [3e] R. N. W. Baxter, J.-M. Lehn, I. Fisher, M.-T. Youinou, *Angew. Chem. Int. Ed. Engl.* **1994**, 33, 2284–2287; *Angew. Chem.* **1994**, 106, 2432–2434. — [3f] D. M. L. Goodgame, S. Menzer, A. M. Smith, D. J. Williams, *J. Chem. Soc., Chem. Commun.* **1994**, 1825–1826. — [3g] L. R. MacGillivray, S. Subramanian, M. J. Zaworotko, *J. Chem. Soc., Chem. Commun.* **1994**, 1325–1326. — [3h] M. Fujita, Y. J. Kwon, M. Miyazawa, K. Ogura, *J. Chem. Soc., Chem. Commun.* **1994**, 1977–1978. — [3i] P. R. Stang, K. Chen, *J. Am. Chem. Soc.* **1995**, 117, 1667–1668. — [3j] D. M. L. Goodgame, S. Menzer, A. M. Smith, D. J. Williams, *Angew. Chem. Int. Ed. Engl.* **1995**, 34, 574–575; *Angew. Chem.* **1995**, 107, 605–607. — [3k] O. M. Yaghi, H. Li, *J. Am. Chem. Soc.* **1996**, 118, 295–296. — [3l] L. D. Sarson, K. Ueda, M. Takeuchi, S. Shinkai, *Chem. Commun.* **1996**, 619–620. — [3m] A. J. Blake, N. R. Champness, S. S. M. Chung, W.-S. Li, M. Schröder, *Chem. Commun.* **1997**, 1005–1006.
- [4] [4a] P. R. Ashton, T. T. Goodnow, A. E. Kaifer, M. V. Reddington, A. M. Z. Slawin, N. Spencer, J. F. Stoddart, C. Vicent, D. J. Williams, *Angew. Chem. Int. Ed. Engl.* **1989**, 28, 1396–1399; *Angew. Chem.* **1989**, 101, 1404–1407. — [4b] C. A. Hunter, J. K. M. Sanders, *J. Am. Chem. Soc.* **1990**, 112, 5525–5534. — [4c] P. R. Ashton, D. Philp, N. Spencer, J. F. Stoddart, D. J. Williams, *J. Chem. Soc., Chem. Commun.* **1994**, 181–184. — [4d] D. B. Amabilino, P. R. Ashton, J. F. Stoddart, S. Menzer, D. J. Williams, *J. Chem. Soc., Chem. Commun.* **1994**, 2475–2478. — [4e] C. A. Hunter, *Chem. Soc. Rev.* **1994**, 101–109. — [4f] R. S. Lokey, B. L. Iverson, *Nature (London)* **1995**, 375, 303–305.
- [5] [5a] G. R. Desiraju, *Crystal Engineering. The Design of Organic Solids*, Elsevier, Amsterdam, **1999**. — [5b] M. C. Etter, *Acc. Chem. Res.* **1990**, 23, 120–126. — [5c] C. B. Aakeröy, K. R. Seddon, *Chem. Soc. Rev.* **1993**, 397–407. — [5d] M. J. Zaworotko, *Chem. Soc. Rev.* **1994**, 283–288. — [5e] G. R. Desiraju, *Angew. Chem. Int. Ed. Engl.* **1995**, 34, 2311–2327; *Angew. Chem.* **1995**, 107, 2541–2558. — [5f] *The Crystal as a Supramolecular Entity* (Ed: G. R. Desiraju), Wiley, New York, **1995**. — [5g] *Comprehensive Supramolecular Chemistry*, vol. 6 (Eds.: J. L. Atwood, J. E. D. Davies, D. D. MacNicol, F. Vögtle), Pergamon, Oxford, **1996**.
- [6] [6a] J.-M. Lehn, *Science* **1993**, 260, 1762–1763. — [6b] F. N. Diederich, *Nature (London)* **1994**, 369, 199–207. — [6c] D. B. Amabilino, J. F. Stoddart, D. J. Williams, *Chem. Mater.* **1994**, 6, 1159–1167. — [6d] V. A. Russel, M. C. Etter, M. D. Ward, *Chem. Mater.* **1994**, 6, 1206–1217. — [6e] N. J. Long, *Angew. Chem. Int. Ed. Engl.* **1995**, 34, 21–38; *Angew. Chem.* **1995**, 107, 37–56.
- [7] A. I. Kitaigorodskii, *Molecular Crystals and Molecules*, Academic Press, New York, **1973**.
- [8] [8a] J. Y. Ortholand, A. M. Z. Slawin, N. Spencer, J. F. Stoddart, D. J. Williams, *Angew. Chem. Int. Ed. Engl.* **1989**, 28, 1394–1396; *Angew. Chem.* **1989**, 101, 1402–1404. — [8b] P. R. Ashton, C. L. Brown, E. J. T. Chrystal, T. T. Goodnow, A. E. Kaifer, K. P. Parry, D. Philp, A. M. Z. Slawin, N. Spencer, J. F. Stoddart, D. J. Williams, *J. Chem. Soc., Chem. Commun.* **1991**, 634–639.
- [9] P.-L. Anelli, M. Asakawa, P. R. Ashton, G. R. Brown, W. Hayes, O. Kocian, S. Rodriguez Pastor, J. F. Stoddart, M. S. Tolley, A. J. P. White, D. J. Williams, *J. Chem. Soc., Chem. Commun.* **1995**, 2541–2545.
- [10] [10a] P. R. Ashton, D. Philp, N. Spencer, J. F. Stoddart, D. J. Williams, *J. Chem. Soc., Chem. Commun.* **1994**, 181–184. — [10b] D. B. Amabilino, P. R. Ashton, J. F. Stoddart, S. Menzer, D. J. Williams, *J. Chem. Soc., Chem. Commun.* **1994**, 2475–2478.
- [11] [11a] O. Dideberg, L. Dupont, J. M. Andre, *Acta Crystallogr., Sect. B* **1972**, 28, 1002–1007. — [11b] A. Banerjee, *Acta Crystallogr., Sect. B* **1973**, 29, 2070–2074. — [11c] C. R. Hubbard, A. D. Mighell, I. H. Pomerantz, *Acta Crystallogr., Sect. B* **1978**, 34, 2381–2384. — [11d] M. Asakawa, P. R. Ashton, C. L. Brown, M. C. T. Fyfe, S. Menzer, D. Pasini, C. Scheuer, N. Spencer, J. F. Stoddart, A. J. P. White, D. J. Williams, *Chem. Eur. J.* **1997**, 3, 1136–1150.
- [12] [12a] P. R. Ashton, C. L. Brown, E. J. T. Chrystal, T. T. Goodnow, A. E. Kaifer, K. P. Parry, A. M. Z. Slawin, N. Spencer, J. F. Stoddart, D. J. Williams, *Angew. Chem. Int. Ed. Engl.* **1991**, 30, 1039–1041; *Angew. Chem.* **1991**, 103, 1055–1058. — [12b] P. R. Ashton, S. E. Boyd, C. G. Claessens, R. E. Gillard, S. Menzer, J. F. Stoddart, M. S. Tolley, A. J. P. White, D. J. Williams, *Chem. Eur. J.* **1997**, 3, 788–797.
- [13] [13a] P. R. Ashton, S. Menzer, F. M. Raymo, G. K. H. Shimizu, J. F. Stoddart, D. J. Williams, *J. Chem. Soc., Chem. Commun.* **1996**, 487–490. — [13b] M. Asakawa, P. R. Ashton, S. Menzer, F. M. Raymo, J. F. Stoddart, A. J. P. White, and D. J. Williams, *Chem. Eur. J.* **1996**, 2, 877–893.
- [14] M. Asakawa, P. R. Ashton, S. E. Boyd, C. L. Brown, S. Menzer, D. Pasini, J. F. Stoddart, M. S. Tolley, A. J. P. White, D. J. Williams, P. G. Wyatt, *Chem. Eur. J.* **1997**, 3, 463–481.
- [15] P. R. Ashton, C. G. Claessens, W. Hayes, S. Menzer, J. F. Stoddart, A. J. P. White, D. J. Williams, *Angew. Chem. Int. Ed. Engl.* **1995**, 34, 1862–1865; *Angew. Chem.* **1995**, 107, 1994–1997.
- [16] B. Odell, M. V. Reddington, A. M. Z. Slawin, N. Spencer, J. F. Stoddart, D. J. Williams, *Angew. Chem. Int. Ed. Engl.* **1988**, 27, 1547–1550; *Angew. Chem.* **1988**, 100, 1605–1608.
- [17] D. B. Amabilino, P.-L. Anelli, P. R. Ashton, G. R. Brown, E. Cordova, L. A. Godinez, W. Hayes, A. E. Kaifer, D. Philp, A. M. Z. Slawin, N. Spencer, J. F. Stoddart, M. S. Tolley, D. J. Williams, *J. Am. Chem. Soc.* **1995**, 117, 11142–11170.
- [18] The mean interplane separation between the bipyridinium and cyclopentadienyl ring systems is 3.4 Å, the vector linking the centroid of the two cyclopentadienyl rings is inclined by 10.5° to the mean plane of the macrocycle.
- [19] R. E. Lehmann, J. K. Kochi, *J. Am. Chem. Soc.* **1991**, 113, 501–512.
- [20] D. D. Perrin, W. L. Armarego, *Purification of Laboratory Chemicals*, 3rd ed., Pergamon Press, New York, **1988**.

[97373]